Bioconjugate Chemistry

pubs.acs.org/bc

Article

Iodine-124 Based Dual Positron Emission Tomography and Fluorescent Labeling Reagents for *In Vivo* Cell Tracking

Truc Thuy Pham, Zhi Lu, Christopher Davis, Chun Li, Fangfang Sun, John Maher, and Ran Yan*

Cite This: *Bioconjugate Chem.* 2020, 31, 1107−1116

Read Online

ACCESS | Metrics & More | Article Recommendations | Supporting Information

ABSTRACT: Understanding the *in vivo* behavior of experimental therapeutic cells is fundamental to their successful development and clinical translation. Iodine-124 has the longest half-life (4.2 days) among the clinically used positron emitters. Consequently, this isotope offers the longest possible tracking time for directly labeled cells using positron emission tomography (PET). Herein, we have radiosynthesized and evaluated two iodine-124/fluorescein-based dual PET and fluorescent labeling reagents, namely ^{124}I-FIT-Mal and ^{124}I-FIT-$(PhS)_2$Mal for cell surface thiol bioconjugation. ^{124}I-FIT-$(PhS)_2$Mal labeled cells significantly more effectively than ^{124}I-FIT-Mal. It conjugated to various cell lines in 22%−62% labeling efficiencies with prolonged iodine-124 retention. ^{124}I-FIT-$(PhS)_2$Mal mainly conjugated on the cell membrane, which was confirmed by high-resolution fluorescence imaging. The migration of ^{124}I-FIT-$(PhS)_2$Mal labeled Jurkat cells was visualized in NSG mice with excellent target-to-background contrast using PET/CT over 7 days. These data demonstrate that ^{124}I-FIT-$(PhS)_2$Mal can dynamically track cell migration *in vivo* using PET/CT over a clinically relevant time frame.

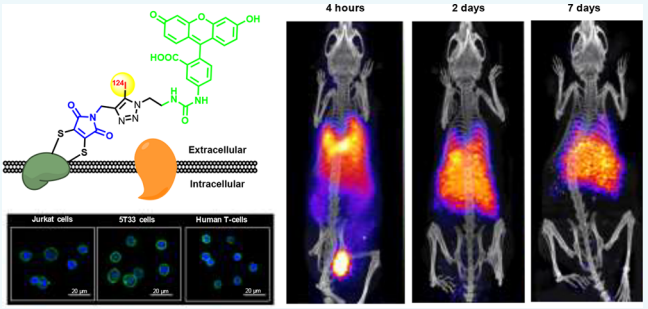

INTRODUCTION

Emerging as the fourth pillar of healthcare, cell-based therapies have shown great promise in cancer treatment,[1] stem cell regenerative medicine,[2] and immune tolerance in organ transplantation.[3] For example, adoptive transfer of chimeric antigen receptor (CAR)-engineered T-cells is a novel immunotherapy that utilizes the patient's own immune system to treat cancer.[4] One fundamental challenge in both medical research and clinical applications of cell therapies is to understand the *in vivo* behavior of the infused cells. Imaging studies can dynamically track the migration, proliferation, and final fate of the administered cells providing early insight into their safety, mechanism of action, and efficacy.[5,6] Therefore, it is essential to incorporate tracking studies at the earliest stage of clinical development in order to monitor the *in vivo* location and persistence of the cells on a patient-by-patient basis.[5,6]

To detect the initial distribution and migration of the infused cells, various direct cell labeling methods have been developed by which the therapeutic cells are labeled with a contrast reagent *in vitro*. Once inoculated into the experimental animals or patients, the movement of the labeled cells can be monitored using the corresponding imaging modality.[7−10] Positron emission tomography (PET) is a noninvasive imaging technique that can produce real-time images of radiolabeled cells *in vivo* and monitor their whole-body migration.[11] Currently, the most successful direct cell labeling method for PET involves the use of lipophilic radiometal complex, ^{89}Zr-$(oxine)_4$ to deposit ^{89}Zr intracellularly.[12,13] Owning to the 3.3 days half-life of ^{89}Zr, this method has been employed to track a variety of cells for several days *in vivo*. Alternatively, an ^{89}Zr-desferrioxamine-isothiocyanate bioconjugation reagent was reported to label cells through the amine groups in cell surface proteins, allowing the assessment of the distribution of the labeled cells *in vivo* for days.[14] However, when applying both of the above ^{89}Zr based cell tracking methods to monitor the experimental therapeutic cells in preclinical settings, the ^{89}Zr leaks gradually from the labeled cells *in vivo* and deposits in bones, complicating the interpretation of PET images.[10,11,13,14]

Iodine-124 has the longest half-life ($t_{1/2}$ = 4.2 d) among the clinically used PET radioisotopes.[15] In principle, it can provide the longest possible tracking time for directly labeled cells with PET. In addition, the thyroid and stomach uptake of any free iodine-124 generated through the catabolism of the labeling reagent can be readily blocked by pretreatment with potassium iodide. Consequently, this approach provides a low background that will improve the sensitivity and accuracy to detect the labeled cells. However, the major challenge with the use of iodine-124 based reagents for direct cell labeling is how to

Received: November 26, 2019
Revised: March 3, 2020
Published: March 4, 2020

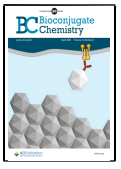

https://dx.doi.org/10.1021/acs.bioconjchem.9b00799
Bioconjugate Chem. 2020, 31, 1107−1116

Scheme 1. Synthesis of the Dual PET and Fluorescent Labeling Reagents[a]

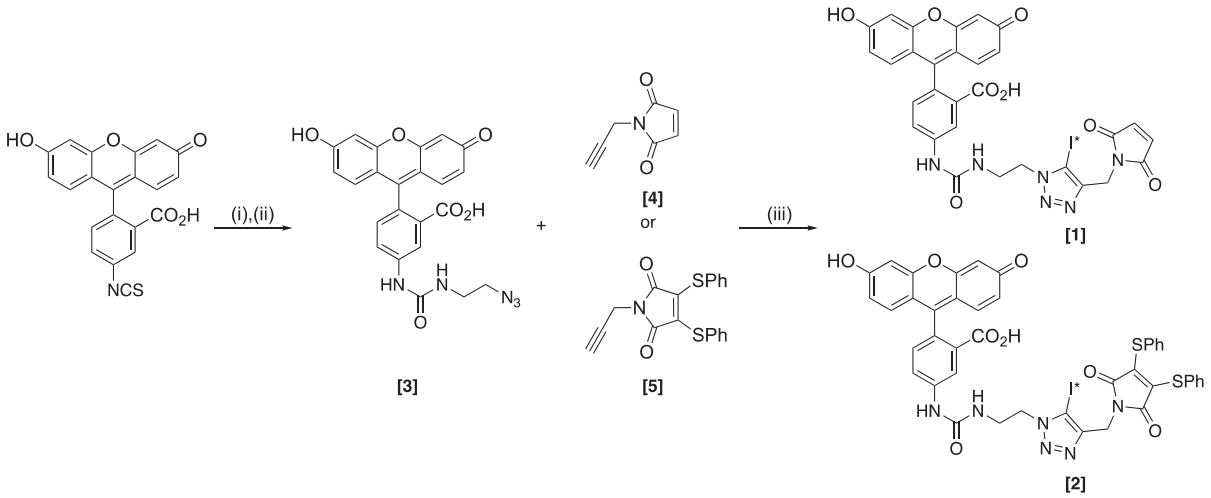

[a](i) 2-Azidoethan-1-amine, TEA, DCM/THF, 0 °C to RT in 3 h, 82%; (ii) pyridinium tribromide (2.0 equiv), THF/H_2O, RT, 3 h, 63%; (iii) a) CuI, TEA, NIS, DMF, 18 h; when I* = ^{127}I or b) $CuCl_2$, TEA/TEA·HCl, bathophenanthroline (10 mol %), [^{124}I]NaI, DMF/CH_3CN/H_2O; when I* = ^{124}I.

overcome various intracellular oxido-reductase-mediated deiodination.[15] We envisage that the deiodination can be minimized by coupling the iodine-124 on the cell surface. For this purpose, we choose thiols present in cell membrane proteins for labeling because they have been proven to be ideal functional groups in various bioconjugation applications.[16,17] To achieve both effective cell conjugation and minimum passive diffusion of labeling reagents into cells, we hypothesize that the labeling reagents should be amphiphiles in nature. In this context, such reagents will be equipped with a lipophilic warhead to reach and react with thiols in the lipid surrounded cell surface proteins. They will also contain a negatively charged hydrophilic moiety that will repulse the negatively charged phosphate heads of the membrane lipids to minimize the labeling reagents diffusing into cells. In addition, a fluorophore will also be employed to confirm effective cell surface conjugation with fluorescence imaging. To achieve these goals, we selected two thiol-targeting moieties, maleimide and dithiophenolmaleimide, for cell surface conjugation. The maleimide reacts irreversibly with the free thiols on the cell surface as demonstrated by others.[16,17] The dithiophenolmaleimide spontaneously reacts with both thiols from the reduced disulfide bridge and preserves the bridge structure in antibodies and peptides.[18,19] Although never having been applied to cell labeling before, we envisaged that these characteristics of dithiophenolmaleimide would enable it to conjugate to the cell surface proteins effectively with minimal adverse effects. We selected fluorescein as the fluorescent reporter for this application since it is used clinically in man and thus should exert negligible toxicity. Moreover, the carboxylic acid group of this hydrophilic dye is deprotonated and becomes negatively charged under physiological pH, which would retard the labeling reagent from entering cells.

Herein, using a copper-mediated one-pot three-component radioiodination reaction,[20−22] we synthesized two trifunctional dual PET and fluorescent bioconjugation reagents, ^{124}I-FIT-Mal [**1**] and ^{124}I-FIT-(PhS)2Mal [**2**]. These are equipped with (i) iodine-124 for longitudinal cell tracking with PET; (ii) a hydrophilic fluorescein moiety to balance lipophilicity and enable fluorescence cell imaging; and (iii) a maleimide or dithiophenolmaleimide moiety for cell membrane protein thiol bioconjugation.

RESULTS

Synthetic Chemistry and Radiolabeling. Initially, the fluorescein isothiocyanate isomer I was reacted with 2-azidoethan-1-amine to generate the 5-[3-(2-azidoethyl)-thioureido]-fluorescein in 82% yield. This was then converted to the 5-[3-(2-azidoethyl)ureido]-fluorescein [**3**] using pyridinium tribromide (2 equiv) in 63% yield.[23] The *N*-propargyl maleimide [**4**][21] and the *N*-propargyl-3,4-dithiophenolmaleimide [**5**][24] were prepared according to published methods. Subsequently, the nonradioactive reference compound of ^{124}I-FIT-Mal [**1**] was synthesized by the copper(I)-mediated one-pot three-component reaction from 5-[3-(2-azidoethyl)-ureido]-fluorescein [**3**], *N*-propargyl maleimide [**4**], and *N*-iodosuccinimide (NIS) in 56% yield. Similarly, the nonradioactive reference compound of ^{124}I-FIT-$(PhS)_2$Mal [**2**] was prepared by reacting 5-[3-(2-azidoethyl)ureido]-fluorescein [**3**] with *N*-propargyl-3,4-dithiophenolmaleimide [**5**] and NIS in 45% yield (Scheme 1).

Next, the ^{124}I-FIT-Mal [**1**] and ^{124}I-FIT-$(PhS)_2$Mal [**2**] were radiosynthesized using a one-pot three-component radioiodination reaction. The 5-[3-(2-azidoethyl)ureido]-fluorescein [**3**] and either *N*-propargyl maleimide [**4**] or *N*-propargyl-3,4-dithiophenolmaleimide [**5**] were reacted with [^{124}I]NaI in a catalytic system of $CuCl_2$/Et_3N/bathophenanthroline (10 mol %) (Scheme 1). Excellent radiochemical yields (RCYs) of 81 ± 6% (n = 6) and 71 ± 1% (n = 7) were obtained for ^{124}I-FIT-Mal [**1**] and ^{124}I-FIT-$(PhS)_2$Mal [**2**], respectively, as determined by HPLC (Figures S1 and S3). The isolated RCYs for ^{124}I-FIT-Mal [**1**] and ^{124}I-FIT-$(PhS)_2$Mal [**2**] were 60 ± 6% (n = 6) and 53 ± 1% (n = 7), respectively. The identities of ^{124}I-FIT-Mal [**1**] and ^{124}I-FIT-$(PhS)_2$Mal [**2**] were confirmed by the coelution with their corresponding nonradioactive reference compounds (Figures S2 and S4). The molar activities of ^{124}I-FIT-Mal [**1**] and ^{124}I-FIT-$(PhS)_2$Mal [**2**] were about 2.30 GBq/μmol and 1.30 GBq/μmol, respectively, when started with ∼10 MBq of iodine-124. The log D for ^{124}I-FIT-Mal [**1**] and ^{124}I-FIT-$(PhS)_2$Mal [**2**] was measured by a

https://dx.doi.org/10.1021/acs.bioconjchem.9b00799
Bioconjugate Chem. 2020, 31, 1107−1116

conventional partition method between n-octanol and pH 7.4 PBS as −0.72 ± 0.02 and 1.42 ± 0.09 (n = 6), respectively.

Cell Radiolabeling Efficiency and Cellular Localization of the Dual Labeling Reagents. Immortalized Jurkat human T cell lymphoma cells (5×10^6) were incubated with ^{124}I-FIT-Mal [**1**] or ^{124}I-FIT-$(PhS)_2$Mal [**2**] in PBS at 37 °C for 30 min. Low labeling efficiencies of 4 ± 1% and 11 ± 1% (n = 3) for ^{124}I-FIT-Mal [**1**] and ^{124}I-FIT-$(PhS)_2$Mal [**2**], respectively, were observed. In parallel experiments, Jurkat cells (5×10^6) were pretreated with tris(2-carboxyethyl)phosphine (TCEP) (1.0 mM), a disulfide bridge reducing reagent in PBS for 15 min. The TCEP was then removed before incubating the cells with ^{124}I-FIT-Mal [**1**] or ^{124}I-FIT-$(PhS)_2$Mal [**2**] in PBS at 37 °C for another 30 min. Significantly increased cell labeling efficiencies of 11 ± 1% and 22 ± 1% (n = 3) for ^{124}I-FIT-Mal [**1**] and ^{124}I-FIT-$(PhS)_2$Mal [**2**], respectively, were achieved (Figure 1A). As ^{124}I-FIT-$(PhS)_2$Mal [**2**] labeled

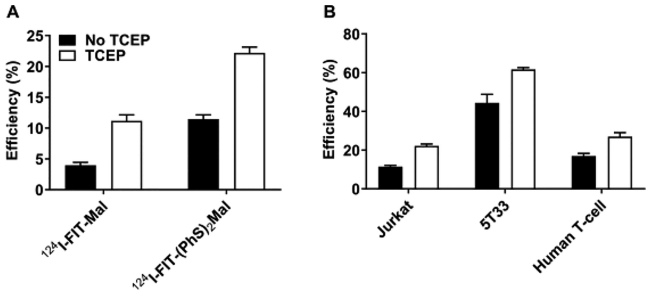

Figure 1. Cell labeling efficiencies of ^{124}I-FIT-Mal [**1**] and ^{124}I-FIT-$(PhS)_2$Mal [**2**] with Jurkat cells (**A**) and cell labeling efficiencies of ^{124}I-FIT-$(PhS)_2$Mal [**2**] with Jurkat, 5T33, and human T-cells (**B**) (% incubation dose per 5×10^6 cells, mean ± SD, n = 3 independent replicates).

Jurkat cells much more effectively than ^{124}I-FIT-Mal [**1**], it was further tested to label murine myeloma 5T33 cells and human peripheral blood T-cells. By pretreating both cell lines (5×10^6) with TCEP and then incubating with ^{124}I-FIT-$(PhS)_2$Mal [**2**], cell labeling efficiencies of 62 ± 1% and 27 ± 2% (n = 3), respectively, were obtained. Once again, lower cell labeling efficiencies of 44 ± 4% and 17 ± 1% (n = 3) for the 5T33 cells and human T-cells, respectively, were observed without TCEP pretreatment (Figure 1B). To investigate the cellular localization of ^{124}I-FIT-$(PhS)_2$Mal [**2**], Jurkat, 5T33, and human T-cells were incubated with the nonradioactive reference compound of ^{124}I-FIT-$(PhS)_2$Mal [**2**] (1.0 μM) after TCEP pretreatment. The labeled cells were then observed under a confocal fluorescence microscope. Green fluorescent signals mainly distributed on the cell membrane for all three cell lines (Figure 2).

Jurkat Cell ^{124}I-Retention, Viability, Proliferation, and Cytokine Release Postradiolabeling. We investigated the retention of iodine-124 by the ^{124}I-FIT-$(PhS)_2$Mal [**2**] labeled Jurkat cells (~100 KBq/10^6 cells) when cultured for 7 days in complete cell medium. ^{124}I-FIT-$(PhS)_2$Mal [**2**] labeled Jurkat cell viability, proliferation, and interleukin-2 (IL-2) release were also monitored and compared with unlabeled Jurkat cells. After an initial rapid loss of about 25% radioactivity in the first 24 h, the dissociation of iodine-124 from the labeled Jurkat cells was very slow. Notably, 65 ± 3% (n = 6) of total radioactivity was still retained in the Jurkat cells 7 days postlabeling (Figure 3A). Cell viability was similar to the unlabeled Jurkat cells as determined by the Trypan Blue

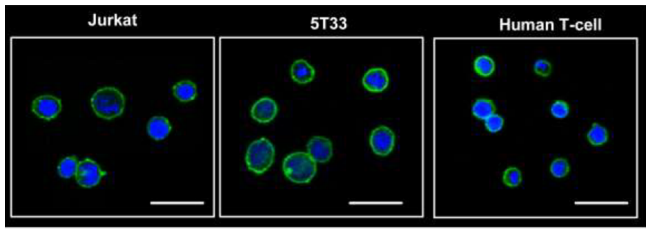

Figure 2. Confocal fluorescence images of the nonradioactive reference compound of ^{124}I-FIT-$(PhS)_2$Mal [**2**] labeled Jurkat, 5T33, and human T-cells. Nuclei were counterstained with Hoechst 33342. (Scale bar = 20 μm.)

exclusion assay (Figure 3B). Proliferation of ^{124}I-FIT-$(PhS)_2$Mal [**2**] labeled Jurkat cells (~100 KBq/10^6 cells) was determined using the CCK-8 assay, which measures the dehydrogenase metabolic activity of proliferating cells. There is no statistically significant difference between the proliferation rates of labeled and unlabeled Jurkat cells over 7 days (Figure 3C). To determine Jurkat cell function postradiolabeling, ^{124}I-FIT-$(PhS)_2$Mal [**2**] labeled (~100 KBq/10^6 cells) or unlabeled Jurkat cells were treated with or without PMA/ionomycin for 24 h. The IL-2 generated was then measured using ELISA. Both labeled and unlabeled Jurkat cells produced comparable amount of IL-2 upon stimulation, while little IL-2 was generated in the absence of PMA/ionomycin (day 6) (Figure 3D).

***In Vivo* Cell Tracking with PET Imaging and Biodistribution Study.** Subsequently, we carried out a tracking study of ^{124}I-FIT-$(PhS)_2$Mal [**2**] labeled Jurkat cells (~0.5−1.0 × 10^7 cells, ~0.5−1.0 MBq) in NSG mice (n = 3) by five sequential PET/CT scans at 4, 24 h, 2, 5, and 7 days postintravenous (IV) injection. Radioactivity accumulated mainly in the lungs, liver, and bladder in the 4 and 24 h PET/CT images. The radioactivity gradually migrated from the lungs to the liver and cleared from the bladder in the NSG mice in the day 2, 5, and 7 PET/CT images (Figure 4A). After completion of PET/CT imaging on day 7, all three animals were euthanized for a biodistribution study. Radioactivity uptake of 7.90 ± 0.88%, 2.94 ± 0.28%, and 2.38 ± 0.74% injected dose (ID)/g was detected in lungs, liver, and spleen, respectively (mean ± SD, n = 3). Radioactivity uptake in other organs such as blood, bone, etc. was all less than 1% ID/g (Figure 5A and Table S1). In the control group, NSG mice (n = 4) received the dual labeling reagent, ^{124}I-FIT-$(PhS)_2$Mal [**2**] IV, and underwent a PET/CT scan after 24 h. Most of the radioactivity had cleared from the animals, and only very weak radioactivity signals were observed in the large intestine and bladder, as shown in the 24 h PET/CT image (Figure 4B). All four animals were euthanized after PET/CT imaging for a biodistribution study. Minimal radioactivity was detected in the lungs (0.88 ± 0.20% ID/g), liver (0.63 ± 0.09% ID/g), and spleen (0.44 ± 0.05% ID/g) of these animals (Figure 5B and Table S2).

***Ex Vivo* Immunohistochemistry Study.** Finally, we undertook immunohistology staining of liver and lung tissues harvested from NSG mice that were inoculated with ^{124}I-FIT-$(PhS)_2$Mal [**2**] labeled Jurkat cells in the PET imaging study. As controls, the liver and lungs from three NSG mice received either PBS or nonlabeled Jurkat cells (~1.0 × 10^7), were collected for immunohistology staining 7 days post IV injection. All tissue sections were sequentially incubated with anti-human CD3 as the primary antibody and polymer-

https://dx.doi.org/10.1021/acs.bioconjchem.9b00799
Bioconjugate Chem. 2020, 31, 1107−1116

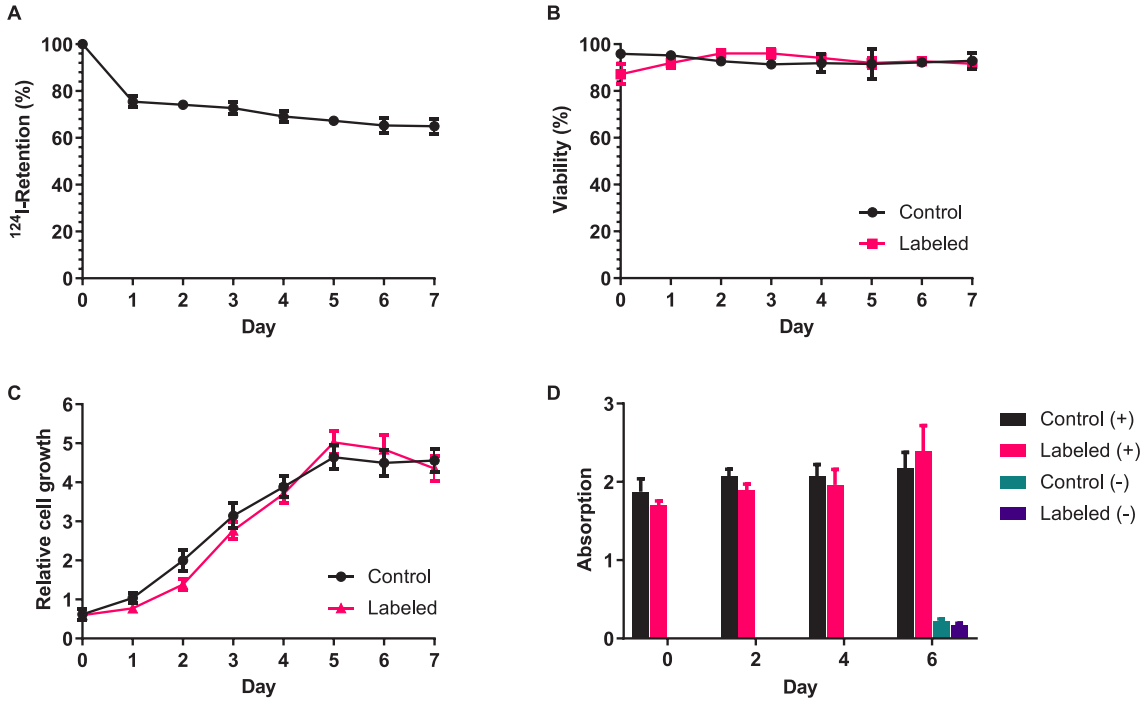

Figure 3. Retention of iodine-124 (**A**), cell viability (**B**), cell proliferation by CCK-8 assay (**C**), and IL-2 production with (+) and without (−) PMA/ionomycin activation by ELISA assay (**D**) of ^{124}I-FIT-$(PhS)_2$Mal [**2**] labeled Jurkat cells (∼100 KBq/10^6 cells, mean ± SD, n = 6 for **A** and **B**; n = 3 for **C** and **D**, independent replicates). Unlabeled cells serve as control.

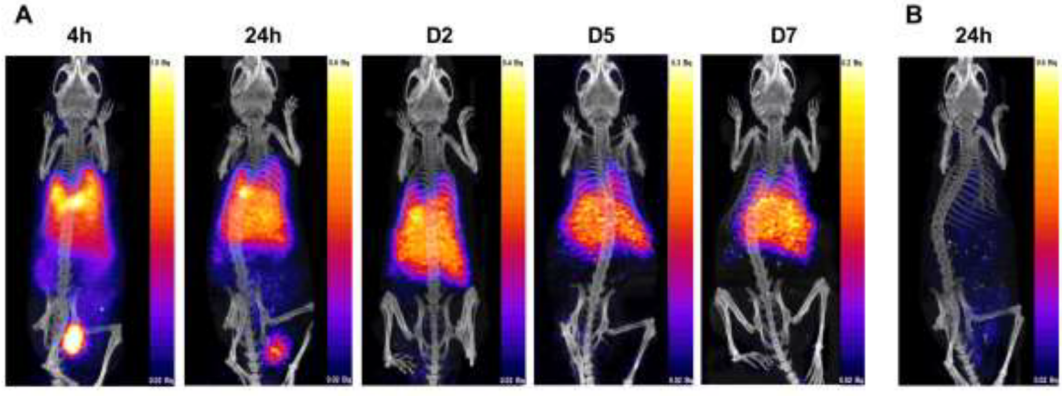

Figure 4. Representative PET/CT images of NSG mice that received either ^{124}I-FIT-$(PhS)_2$Mal [**2**] labeled Jurkat cells at 4, 24 h, 2, 5, and 7 days (n = 3) (**A**) or ^{124}I-FIT-$(PhS)_2$Mal [**2**] at 24 h post IV injection (n = 4) (**B**). All animals were treated with potassium iodide 1 week before and throughout the PET/CT imaging experiments.

supported peroxidase/anti-Mouse IgG as followed by the 3,3′-diaminobenzidine (DAB) treatment. Both ^{124}I-FIT-$(PhS)_2$Mal [**2**] labeled and nonlabeled Jurkat cells migrated to the liver and lung tissues from the NSG mice either used in the PET imaging study or the positive control group were stained brown in color (Figure 6, labeled or nonlabeled Jurkat). In contrast, the anti-human CD3 staining was negative in the liver and lung tissues from the PBS-treated NGS mice in the negative control group (Figure 6, PBS).

DISCUSSION

Initially, the nonradioactive reference compounds of ^{124}I-FIT-Mal [**1**] and ^{124}I-FIT-$(PhS)_2$Mal [**2**] were synthesized in moderate yields using copper-mediated one-pot three-component click reactions. It proved essential to use 5-[3-(2-azidoethyl)ureido]-fluorescein [**3**] rather than its corresponding 5-[3-(2-azidoethyl)thioureido]-fluorescein formed in the first synthetic step in Scheme 1. No desired iodotriazoles were formed when 5-[3-(2-azidoethyl)thioureido]-fluorescein was used. This is because thioureas are susceptible to copper(II) oxidation.[25] In terms of radiosynthesis, a longer reaction time of 18 h at RT was required to prepare ^{124}I-FIT-Mal [**1**] in both excellent RCYs and molar activity. When radiolabeling was attempted at elevated temperature, the formation of both radioactive and nonradioactive side products was observed, which significantly reduced the RCYs and molar activity of ^{124}I-FIT-Mal [**1**]. As iodine-124 has a half-life of 4.2 days, we decided to adopt the longer reaction time for the preparation of ^{124}I-FIT-Mal [**1**]. In contrast, ^{124}I-FIT-$(PhS)_2$Mal [**2**] was formed in both excellent RCYs and molar activity in 90 min which allows its production, cell labeling, and subsequent biological evaluation in a clinically relevant time frame. Control

https://dx.doi.org/10.1021/acs.bioconjchem.9b00799
Bioconjugate Chem. 2020, 31, 1107−1116

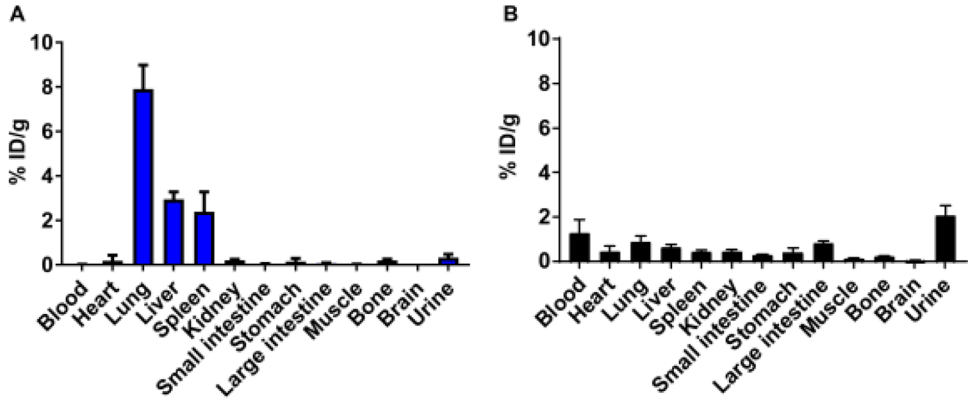

Figure 5. Biodistribution analysis of NSG mice that received either ^{124}I-FIT-(PhS)$_2$Mal [**2**] labeled Jurkat cells on day 7 post IV injection (mean ± SD, n = 3) (**A**) or ^{124}I-FIT-(PhS)$_2$Mal [**2**] at 24 h post IV injection (mean ± SD, n = 4) (**B**). All animals were treated with potassium iodide 1 week before until the day of the biodistribution study.

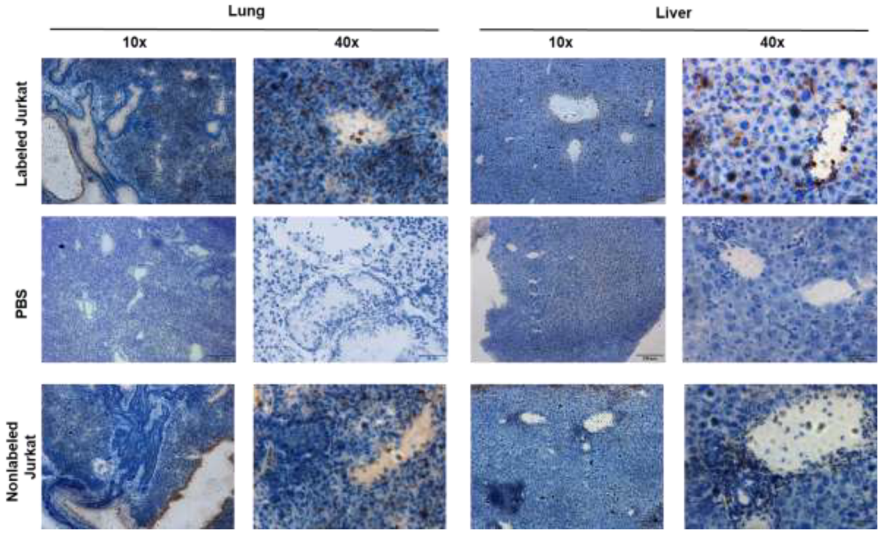

Figure 6. Representative immunohistochemistry images: liver and lung tissues collected from the NSG mice (n = 3) received either ^{124}I-FIT-(PhS)$_2$Mal [**2**] labeled Jurkat cells, PBS, or nonlabeled Jurkat cells 7 days post IV injection. Tissue sections were counterstained with hematoxylin. (Scale bar = 200 μm for 10× or 50 μm for 40×.)

radiolabeling experiments in the absence of the alkynes [**4**] and [**5**] were also conducted, and only the free iodine-124 was observed, which indicated that the phenolic ring of the fluorescein moiety cannot be radioiodinated under the conditions used to prepare both dual labeling reagents.

Subsequently, we investigated Jurkat cell conjugation with ^{124}I-FIT-Mal [**1**] and ^{124}I-FIT-(PhS)$_2$Mal [**2**] with or without pretreatment of the cells using a mild reducing agent, TCEP. It has been used to increase cell surface free thiols for maleimide conjugation on various cell lines including stem cells and cancer cells without adverse effect on cell functions.[16,26] The cell labeling efficiencies achieved for both ^{124}I-FIT-Mal [**1**] and ^{124}I-FIT-(PhS)$_2$Mal [**2**] were significantly improved by pretreating the cells with TCEP which boosts the amount of cell membrane free thiols. The cell labeling efficiency for ^{124}I-FIT-(PhS)$_2$Mal [**2**] was 1-fold higher than that of ^{124}I-FIT-Mal [**1**]. One possible reason is that ^{124}I-FIT-(PhS)$_2$Mal [**2**] is lipophilic which makes it more accessible to lipid surrounded cell membrane proteins. In contrast, the hydrophilic nature of ^{124}I-FIT-Mal [**1**] would be expected to repel it from the cell membrane. The general utility of ^{124}I-FIT-(PhS)$_2$Mal [**2**] for cell labeling was subsequently demonstrated by its successful conjugation to the murine myeloma 5T33 cells and to human peripheral blood T-cells. Significantly higher cell labeling efficiency was observed for the 5T33 cells compared to Jurkat cells and human T-cells. This is likely due to the higher numbers of thiols associated with 5T33 cell surface proteins as determined by the DTNB assay (Supporting Information). The cell membrane localization of ^{124}I-FIT-(PhS)$_2$Mal [**2**] on all three cell lines was confirmed by confocal fluorescence imaging. Despite its lipophilic nature, the ^{124}I-FIT-(PhS)$_2$Mal [**2**] was mainly deposited on the cell membrane. This is likely resulting from the amphiphilic characteristics of this molecule. The fluorescein moiety in ^{124}I-FIT-(PhS)$_2$Mal [**2**] is negatively charged due to the deprotonation of its carboxylic acid group in PBS (pH 7.4), which repels this part of the molecule from the negatively charged cell membrane. Meanwhile, the lipophilic dithiophenolmaleimide moiety in ^{124}I-FIT-(PhS)$_2$Mal [**2**] is attracted by the cell membrane lipids. These combined forces allow ^{124}I-FIT-(PhS)$_2$Mal [**2**] to reach cell membrane protein thiols for conjugation rather than rapidly entering the cells through passive diffusion. Moreover, ^{124}I-FIT-(PhS)$_2$Mal [**2**] has shown remarkable radiolabel

https://dx.doi.org/10.1021/acs.bioconjchem.9b00799
Bioconjugate Chem. 2020, 31, 1107−1116

retention at a radioactivity level of 100 KBq/10^6 Jurkat cells, with minimum effect on cell viability. About 65% of radioactivity was still associated with the Jurkat cells *in vitro* even 7 days postradiolabeling with ^{124}I-FIT-$(PhS)_2$Mal [**2**]. This level of radioactivity retention and tolerance is comparable with that observed following ^{89}Zr(oxine)$_4$ labeling of CAR T-cells. In those cases, 40−80% of ^{89}Zr was retained for 5−7 days postlabeling, while tolerated radioactivity doses ranged from 30 to 70 KBq/10^6 cells.[10−13] Notably, about 25% of the radioactivity was lost in the first 24 h postlabeling followed by the very slow loss of radiolabel from the Jurkat cells, about 7% in 6 days. Due to the lipophilicity of ^{124}I-FIT-$(PhS)_2$Mal [**2**], it would be expected to interact noncovalently with cell membrane lipids which would cause rapid dissociation of ^{124}I-FIT-$(PhS)_2$Mal [**2**] from the cells. In contrast, covalently bonded ^{124}I-FIT-$(PhS)_2$Mal [**2**] showed greater stability. In addition, faint green signals were observed inside the cells in the confocal fluorescence images (Figure 3) indicating a small portion of ^{124}I-FIT-$(PhS)_2$Mal [**2**] did enter the cells, which could also rapidly diffuse out of the cells through passive diffusion.

Jurkat cells are leukemic T-cells that produce IL-2 upon PMA/ionomycin stimulation. When labeled with ^{124}I-FIT-$(PhS)_2$Mal [**2**] at a radioactivity dose of about 100 KBq/10^6 cells, IL-2 production was similar to that of unlabeled control Jurkat cells. In addition, cell proliferation was also largely unaffected post ^{124}I-FIT-$(PhS)_2$Mal [**2**] labeling. Thus, Jurkat cell functions, in terms of IL-2 production and cell proliferation, were reserved at this radioactivity dose.

In the proof of concept *in vivo* tracking study, the migration of ^{124}I-FIT-$(PhS)_2$Mal [**2**] labeled Jurkat cells from the lungs to the liver was clearly visualized in NSG mice using five consecutive PET scans over 7 days. Spleen is a major cell migration organ we expected to observe in PET. However, the high liver radioactivity uptake and the anatomical proximity between liver and spleen completely obscured the spleen in the PET images. It is worth noting that in contrast to the high bone uptake of ^{89}Zr-based cell tracking reagents,[10,11,13,14] no bone uptake was observed in all five PET images from 4 h until 7 days post IV injection of ^{124}I-FIT-$(PhS)_2$Mal [**2**] labeled Jurkat cells. This illustrates the superiority of this iodine-124 based strategy over the current zirconium-89 methods for direct cell labeling and long-term cell tracking with PET. As expected, thyroid and stomach uptake of iodine-124 were completely blocked by treating the animals with potassium iodide, generating a clear background for visualizing cell migration. Moreover, the initial dissociation of the labeling reagent from the Jurkat cells was observed in the 4 and 24 h PET images, as indicated by the accumulation of radioactivity in the bladder. However, little radioactivity was observed in the bladder at later time points (2, 5, and 7 days), indicating that the labeling reagent was still associated with the Jurkat cells. These observations are in good agreement with the *in vitro* iodine-124 retention from the ^{124}I-FIT-$(PhS)_2$Mal [**2**] labeled Jurkat cells. The biodistribution study undertaken on NSG mice 7 days post-inoculation of ^{124}I-FIT-$(PhS)_2$Mal [**2**] labeled Jurkat cells also provided strong evidence that the radioactivity was still concentrated in the organs to which the cells migrated. These include the lungs, liver, and spleen, with little radioactivity detected in other organs at this late time point. In contrast, in the control group that received ^{124}I-FIT-$(PhS)_2$Mal [**2**], both PET/CT imaging and a biodistribution study confirmed that most of the radioactivity was cleared from the NSG mice within 24 h post IV injection. Moreover, the presence of Jurkat cells in the lungs and liver of the NSG mice that received ^{124}I-FIT-$(PhS)_2$Mal [**2**] labeled Jurkat cells from the PET imaging was further confirmed using anti-human CD3 antibody in an *ex vivo* immunohistology staining study. The distribution patterns of the ^{124}I-FIT-$(PhS)_2$Mal [**2**] labeled Jurkat cells in the lung and liver tissues were similar to the nonlabeled Jurkat cells in the positive control group shown by the immunohistology staining study, which hints that the *in vivo* movability of Jurkat cells was reserved post ^{124}I-FIT-$(PhS)_2$Mal [**2**] labeling.

One possible concern is the low radioactivity dose of ^{124}I-FIT-$(PhS)_2$Mal [**2**] (∼100 KBq/10^6 cells) used in the *in vivo* cell tracking study, which might be a limitation to translate this new method to clinical applications. Although there is no clinical PET imaging data to indicate the optimal radioactivity dose for directly labeled cell tracking in human, one ongoing clinical trial employs 7.4−18.5 MBq of ^{89}Zr-labeled leukocytes to track peripheral immune cell infiltration of the brain in patients with central inflammatory disorders over 6 days.[27] Moreover, in a recent ^{89}Zr-labeled natural killer (NK) cell (∼1.5 × 10^8) tracking study in rhesus macaques (∼6.6 kg), clear PET images were acquired with only 2.0 MBq of radioactivity over 7 days.[28]

Given the very similar positron abundance of iodine-124 (22.5%) and zirconium-89 (22.7%), longer half-life of iodine-124 (4.2 days) than zirconium-89 (3.3 days), and excellent iodine-124 retention of ^{124}I-FIT-$(PhS)_2$Mal [**2**] labeled cells, it is a reasonable estimation that this novel iodine-124 based cell labeling method could provide a sufficient radioactivity dose (∼20 MBq in 2 × 10^8 cells) for directly labeled cell tracking with PET in clinical trials.

Additionally, the latest ultrasensitive total-body PET scanner requires a very low radioactivity dose to achieve the same signal-to-noise ratio comparing to the current clinical PET scanners. For example, in the first human PET imaging study with the EXPLORER Total-Body PET Scanner, high quality full-body PET images were acquired by using only 25 MBq of ^{18}F-FDG (1/15 of the normal radioactivity dose) in 10 min.[29] Therefore, we anticipate that the radioactivity dose will not be a barrier to translate ^{124}I-FIT-$(PhS)_2$Mal [**2**] to clinical cell tracking.

CONCLUSION

Two dual PET and fluorescent labeling reagents, ^{124}I-FIT-Mal [**1**] and ^{124}I-FIT-$(PhS)_2$Mal [**2**], were prepared in excellent RCYs and evaluated for cell conjugation. The cell labeling efficiency of ^{124}I-FIT-$(PhS)_2$Mal [**2**] is significantly better than ^{124}I-FIT-Mal [**1**]. ^{124}I-FIT-$(PhS)_2$Mal [**2**] successfully labeled various cell lines through their membrane thiols in 22%−62% labeling efficiency with prolonged radiolabel retention. Cell membrane localization of ^{124}I-FIT-$(PhS)_2$Mal [**2**] was confirmed by confocal fluorescence imaging. Longitudinal monitoring of the *in vivo* distribution and migration of ^{124}I-FIT-$(PhS)_2$Mal [**2**] labeled Jurkat cells was achieved with PET/CT imaging over 7 days with excellent target-to-background contrast. These promising results warrant future studies in which therapeutic cells such as anticancer CAR T-cells will be labeled with ^{124}I-FIT-$(PhS)_2$Mal [**2**] for *in vivo* tracking using PET/CT.

https://dx.doi.org/10.1021/acs.bioconjchem.9b00799
Bioconjugate Chem. 2020, 31, 1107−1116

EXPERIMENTAL SECTION

Synthetic Chemistry and Radiochemistry. *General Information.* ^{1}H and ^{13}C NMR spectra were recorded at RT on a Bruker Avance 400 instrument operating at the frequency of 400 MHz for ^{1}H and 100 MHz for ^{13}C. Chemical shifts are reported in ppm relative to chloroform (δ 7.26, s), dimethyl sulfoxide (δ 2.48, m), or methanol (δ 3.49, s and 1.09, s), and coupling constants (J) are given in Hertz. HPLC analysis was performed with an Agilent 1200 HPLC system equipped with a 1200 series diode array detector. Radio-HPLC analysis was performed with an Agilent 1200 HPLC system equipped with a series diode array detector and Raytest GABI Star radioactivity detector. The radiochemical purity of ^{124}I-FIT-Mal and ^{124}I-FIT-(PhS)$_2$Mal was determined using radioHPLC, and both were greater than 95% (Figures S2 and S4). Reductant free [^{124}I]NaI was purchased from PerkinElmer (product number NEZ309) in 0.02 M NaOH (pH 14) aqueous solution. All reagents were purchased from Sigma-Aldrich and were used without further purification.

5-[3-(2-Azidoethyl)thioureido]-fluorescein. To a solution of fluorescein isothiocyanate isomer I (0.50 g, 1.28 mmol) in anhydrous THF (45 mL) at 0 °C was added the freshly prepared 2-aminoethyl azide[21] solution in DCM (5 mL) under an atmosphere of N_2, followed by triethylamine (0.18 mL, 1.28 mmol). The reaction solution was warmed to RT while stirring for 3 h. The solvents were removed in vacuo, and the residue was purified by column chromatography (DCM, 0.1% TFA → DCM, 5% MeOH, 0.1% TFA) to afford the title compound as a yellow solid (0.51 g, 82%).

^{1}H NMR (400 MHz, MeOH-*d4*): δ 8.17 (1H, s, Ar−CH), 7.79 (1H, J = 8.0 Hz, d, Ar−CH), 7.19 (1H, J = 8.0 Hz, d, Ar−CH), 6.72 (2H, J = 8.0 Hz, d, Ar−CH), 6.68 (2H, J = 4.0 Hz, d, Ar−CH), 6.58 (2H, J = 8.0 Hz, J' = 4.0 Hz, dd, Ar−CH), 3.83 (2H, J = 12.0 Hz, t, CH_2), 3.61 (2H, J = 12.0 Hz, t, CH_2); ^{13}C NMR (100 MHz, DMSO-*d6*) δ 180.8, 168.7, 162.9, 152.9, 141.0 129.3, 128.1, 125.1, 118.2, 114.4, 110.4, 102.3, 49.3, 40.6; HRMS (EI, m/z) [M + H]$^+$: calc. for $C_{23}H_{18}N_5O_5S$ 476.1029; found: 476.1028.

5-[3-(2-Azidoethyl)ureido]-fluorescein [3]. To a solution of 5-[3-(2-azidoethyl)thioureido]-fluorescein (140 mg, 0.3 mmol) and pyridinium tribromide (190 mg, 0.60 mmol) in THF (4 mL) was added dropwise water (2 mL), and the resulting solution was stirred at RT for 3 h. The reaction mixture was filtered. Water (20 mL) was added to the filtrate and extracted with EtOAc (3 × 20 mL). The organic extracts were dried over $MgSO_4$ and evaporated under vacuo. Purification by column chromatography (0−5% MeOH in DCM, 0.1%TFA) yielded the title compound as an orange solid (81 mg, 63%).

^{1}H NMR (400 MHz, DMSO-*d6*): δ 10.08 (2H, s, OH), 9.11 (1H, s, NH), 8.15 (1H, s, Ar−CH), 7.63 (1H, J = 8.0, d, Ar−CH), 7.13 (1H, J = 8.0 Hz, d, Ar−CH), 6.67 (2H, s, Ar−CH), 6.56−6.51 (5H, m, Ar−CH × 4 and NH), 3.46−3.43 (2H, m, CH_2), 3.36−3.33 (2H, m, CH_2); ^{13}C NMR (100 MHz, DMSO-*d6*) δ 169.3, 159.9, 155.6, 152.4, 145.4, 142.5, 129.5, 127.5, 125.7, 124.7, 113.0, 112.2, 110.4, 102.7, 83.4, 51.1, 40.0; HRMS (EI, m/z) [M + H]$^+$: calc. for $C_{23}H_{18}N_5O_6$ 460.1257; found: 460.1267.

Nonradioactive Reference Compounds of the Dual PET and Fluorescent Labeling Reagents. To a solution of copper(I) iodide (14.5 mg, 76.2 μmol) and triethylamine (10.6 μL, 76.2 μmol) in dry DMF (1.0 mL) was added bathophenanthroline (2.5 mg, 7.62 μmol) under an atmosphere of argon, followed by either *N*-propargyl maleimide [**4**] or *N*-propargyl-3,4-dithiophenolmaleimide [**5**] (76.2 μmol), *N*-iodosuccinimide (25.7 mg, 114.4 μmol), and the 5-[3-(2-azidoethyl)ureido]-fluorescein [**3**] (76.2 μmol). The resulting mixture was stirred at RT for 18 h. Water (10 mL) was added, and the product mixture was extracted with EtOAc (3 × 15 mL). The organic extracts were washed with brine and dried over $MgSO_4$. After filtration, the solvent was removed under vacuo.

^{127}I-FIT-Mal [1]. The crude mixture was washed with cold diethyl ether (3 × 10 mL) and then purified with flash column chromatography on silica (0−10% MeOH in DCM) to yield the title compound as an orange solid (31 mg, 56%). ^{1}H NMR (400 MHz, DMSO-*d6*) δ 10.11 (2H, s, OH), 9.24 (1H, s, NH), 8.14 (1H, s, Ar−H), 7.61 (1H, J = 8.0 Hz, d, Ar−H), 7.12 (2H, s, CH = CH), 7.10 (1H, J = 8.0 Hz, d, Ar−H), 6.68 (2H, s, Ar−H) 6.58−6.53 (5H, m, Ar−CH × 4 and NH), 4.62 (2H, s, CH_2), 4.47 (2H, J = 6.0 Hz, t, CH_2); 3.57 (2H, J = 6.0 t, CH_2). ^{13}C NMR (100 MHz, DMSO-*d6*) δ 170.8, 169.3, 159.9, 155.6, 152.4, 146.1, 145.4, 142.5, 135.3, 130.0, 129.5, 127.4, 125.7, 124.6, 113.0, 112.2, 110.4, 102.7, 83.5, 83.4, 55.4, 50.3, 46.0. HRMS (EI, m/z) [M + H]$^+$: calc. for $C_{30}H_{22}IN_6O_8$ 721.0544; found 721.0533.

^{127}I-FIT-(PhS)$_2$Mal [2]. The crude product was purified by C-18 reverse phase flash column chromatography using Combiflash (5−95% MeOH in water) to afford the title compound as an orange solid (32 mg, 45%).

^{1}H NMR (400 MHz, DMSO-*d6*) δ 9.15 (1H, s, NH), 8.14 (1H, J = 2.0 Hz, d, Ar−H), 7.60 (1H, J = 8.0 Hz, J' = 2.0 Hz, dd, Ar−H), 7.34−7.23 (10H, m, Ph × 2), 7.11 (1H, J = 8.0 Hz, d, Ar−H), 6.67 (2H, J = 2.0, d, Ar−H), 6.74−6.43 (4H, m), 6.48 (1H, J = 11.0 Hz, t, NH), 4.65 (2H, s), 4.48 (2H, J = 6.0 Hz, t); 3.58 (2H, J = 11.0 Hz, J' = 6.0 Hz, q). ^{13}C NMR (100 MHz, DMSO-*d6*) δ 168.9, 165.7, 159.4, 155.0, 151.9, 145.1, 144.9, 142.0, 135.8, 130.9, 130.9, 129.1, 129.0, 128.9, 128.1, 126.9, 125.3, 124.2, 112.5, 111.7, 109.9, 102.1, 82.9, 82.8, 49.8, 34.4; HRMS (EI, m/z) [M + H]$^+$: calc. for $C_{42}H_{30}IN_6O_8S_2$ 937.0611, found: 937.0635.

Radiolabeling. Copper(II) chloride (3.4 mg, 25.3 μmol), triethylamine (4.4 μL, 31.5 μmol, 1.38 equiv), and bathophenanthroline (850 μg, 2.5 μmol, 10% mol) were mixed in anhydrous acetonitrile (500 μL). The resulting suspension (62.5 μL) was added to either *N*-propargyl maleimide [**4**] or *N*-propargyl-3,4-dithiophenolmaleimide [**5**] (3.1 μmol) in anhydrous DMF (62.5 μL). The resulting red suspension (40 μL) was added to a mixture of 5-[3-(2-azidoethyl)ureido]-fluorescein [**3**] (1.0 μmol) and triethylamine hydrochloride (TEA·HCl) (16.5 μg, 0.12 μmol) in acetonitrile (20 μL) and [^{124}I]NaI (~12 MBq) in 0.02 M NaOH solution (6.0 μL).

^{124}I-FIT-Mal [1]. After incubation at RT for 18 h, the reaction mixture was quenched with DMSO (100 μL) followed by water/MeOH (4:1, 1.0 mL). The resulting solution was purified by HPLC using a ZORBAX column (300SB-C18, 9.4 × 250 mm, 5 μm) with the following eluent: water (0.1% TFA) as solvent A and methanol (0.1% TFA) as solvent B, went from 30% B to 47.5% B in 5 min, kept at 47.5% B for 20 min, went to 90% B in 5 min, and went back to 30% B in 5 min with a flow rate of 2.5 mL/min. The retention time of the title compounds was 20.4 min.

^{124}I-FIT-(PhS)$_2$Mal [2]. After incubation at 60 °C for 90 min, the reaction mixture was quenched with DMSO (100 μL) followed by water/MeOH (4:1, 1.0 mL). The resulting

https://dx.doi.org/10.1021/acs.bioconjchem.9b00799
Bioconjugate Chem. 2020, 31, 1107−1116

solution was purified by HPLC using a ZORBAX column (300SB-C18, 9.4 × 250 mm, 5 μm) with the following eluent: water (0.1% TFA) as solvent A and methanol (0.1% TFA) as solvent B, went from 70% B to 75% B in 15 min, increased to 90% B in 5 min, and went back to 70% B in 5 min with a flow rate of 2.5 mL/min. The retention time of the title compounds was 12.4 min.

The identity of both dual labeling reagents was confirmed by coeluting with their corresponding nonradioactive reference compounds (Figures S2 and S4). Formulation: the HPLC eluent containing the dual labeling reagent was diluted to 15% MeOH in water and was loaded on either a preconditioned Waters C18 light Sep-Pak cartridge for ^{124}I-FIT-Mal [**1**] or Waters t-C18 Sep-Pak cartridge for ^{124}I-FIT-$(PhS)_2$Mal [**2**]. After washing with water (5 mL), the dual labeling reagent was released using EtOH. The EtOH was removed by a stream of N_2, and then the dual labeling reagent was redissolved in DMSO for further use.

Log D Measurement. The lipophilicity of ^{124}I-FIT-Mal [**1**] and ^{124}I-FIT-$(PhS)_2$Mal [**2**] was determined by a conventional partition method between n-octanol and PBS, pH 7.4. The n-octanol was saturated with PBS before use. The ^{124}I-FIT-Mal [**1**] or ^{124}I-FIT-$(PhS)_2$Mal [**2**] (1 μL, ∼ 2 KBq) in DMSO was added to a mixture of PBS (200 μL) and n-octanol (200 μL) in a 1.5 mL Eppendorf vial (n = 6). The mixture was vigorously agitated at RT for 5 min and then centrifuged at 3000 g for 10 min. A 100 μL aliquot from each layer was drawn for measurement using a gamma counter.

Cell Culture. T-cells were isolated from peripheral blood samples taken from healthy volunteers aged 18−45 (KCL ethics approval: HR-18/19-8846) *via* Ficoll separation. Blood was slowly added to a 50 mL Falcon tube containing 15 mL of Ficoll-Paque (GE Healthcare) solution and spun in a centrifuge at 500 g for 25 min. The peripheral blood mononuclear cell layer was extracted, and the cells were washed twice with PBS and prepared for activation. Cells were resuspended in RPMI 1640 cell growth medium at a concentration of 3 × 10^6 cells/mL and plated on a 6-well plate (4 mL per well). T-cells were activated with 5 μg/mL of phytohemagglutinin (PHA-L, Sigma-Aldrich). IL-2 (100 U/mL, PeproTech) and fresh medium were added every 2−3 days.

Jurkat and murine myeloma 5T33 (generous gift from Dr. Yolanda Calle-Patino) cells were cultured in RPMI-1640 medium supplemented with 10% FBS, 200 U/L penicillin, 0.1 g/L streptomycin, and 2 mM L-glutamine. The cell concentration was maintained in 1 × 10^5−1 × 10^6 cells/mL in a humidified chamber containing 5% CO_2 at 37 °C.

Cell Labeling. For ^{124}I-FIT-Mal [**1**] and ^{124}I-FIT-$(PhS)_2$Mal [**2**]: suspension cells (5 × 10^6, n = 3) were either treated with TCEP (1.0 mL, 1.0 mM) in PBS or PBS (1 mL) only and kept at RT for 15 min before washing with PBS (3 × 1.0 mL). The cells were resuspended in PBS (0.5 mL) and followed by the addition of ^{124}I-FIT-Mal [**1**] or ^{124}I-FIT-$(PhS)_2$Mal [**2**] (∼3 MBq) in DMSO (5 μL). After incubation at 37 °C for another 30 min, the cells were centrifuged (1200 rpm, 5 min), and the supernatants were transferred to new Eppendorf tubes. The pellets were further rinsed with PBS (2 × 0.5 mL) before being transferred to new Eppendorf tubes and recultivated in complete medium. To determine the cell labeling efficiency, the supernatants and the washes for each sample were combined. The pellets, supernatants, and Eppendorf tubes used for cell labeling were measured by a Capintec CRC-25R dose calibrator (Capintec Inc., USA).

For the nonradioactive reference compound of ^{124}I-FIT-$(PhS)_2$Mal [**2**]: suspension cells (2 × 10^6, n = 3) were treated with TCEP (1.0 mL, 1.0 mM) in PBS and incubated at RT for 15 min before being washed with PBS (3 × 1.0 mL) to remove TCEP. The cells were then resuspended in PBS (1.0 mL), and the nonradioactive reference compound of ^{124}I-FIT-$(PhS)_2$Mal [**2**] in DMSO (0.5 μL, 2.0 mM) was added to achieve the final concentration of 1.0 μM. The cells were incubated at 37 °C for another 30 min. Hoechst 33342 in DMSO (2 μL, 250 μM) was added to the cells 5 min before the end of incubation. The cells were centrifuged (1200 rpm, 5 min), the supernatants were removed, and the pellets were further rinsed with PBS (3 × 1.0 mL). The sample was then fixed with 4% paraformaldehyde at RT for 10 min in darkness. Following the fixation step, the cells were washed with PBS (3 × 1.0 mL) and resuspended in PBS (50 μL). The cell sample (10 μL) was mounted on a microscopic glass slide, covered with a coverslip, and sealed with transparent nail enamel. High-resolution confocal fluorescence images were obtained with a Leica TCS SP5 II confocal microscope (Leica Microsystems Ltd.) system and processed using LAS AF Lite (ver 2.6.3, build 8173, Leica Microsystems Ltd.). Excitation/emission wavelengths were 495/517 nm and UV/455 nm for FITC and Hoechst 33342, respectively.

Iodine-124 Retention and Cell Viability Postradiolabeling. Both the ^{124}I-FIT-$(PhS)_2$Mal [**2**] labeled and untreated control Jurkat cells were maintained at 0.2−1.0 × 10^6 cells/mL in complete cell media. To determine the retention of iodine-124, the ^{124}I-FIT-$(PhS)_2$Mal [**2**] labeled Jurkat cells (0.5 mL) were collected daily. After centrifugation at 1500 rpm for 5 min, the supernatant and the pellet were separated and gamma counted using a Wallac Wizard 1480 automatic gamma counter (PerkinElmer, USA). Trypan Blue was employed to measure the cell viability. The number of live and dead cells was counted, and the percentage of the cell viability was calculated. The experiments were conducted in triplicates. The data were analyzed using GraphPad Prism 7 software.

Cell Proliferation Assay. The effect of radiolabeling on cellular proliferation was assessed using the Cell Counting Kit-8 (CCK-8). Both the ^{124}I-FIT-$(PhS)_2$Mal [**2**] labeled (∼100 KBq/10^6 cells) and unlabeled Jurkat cells were maintained in complete cell media at an initial concentration of 0.2 × 10^6 cells/mL. The culture medium was replaced daily. The CCK-8 assay was performed in triplicate daily for 7 days. In general, 10 μL of the CCK-8 solution was added to 100 μL aliquots of either the labeled or unlabeled Jurkat cells; then the absorbance at 450 nm was measured with a SpectraMax 190 absorbance microplate reader (Molecular Devices, USA) after incubation at 37 °C for 3 h. The experiments were conducted in triplicate. Results are presented as mean ± SD.

Cell Function Assay. Both the ^{124}I-FIT-$(PhS)_2$Mal [**2**] labeled (∼100 KBq/10^6 cells) and unlabeled Jurkat cells were maintained at 0.2−1.0 × 10^6 cells/mL in complete cell media. The labeled or unlabeled Jurkat cells (1.0 × 10^6 cells/mL) were seeded into a 96 well-plate (100 μL/well) in triplicate. 12-*O*-Tetradecanoylphorbol 13-acetate (PMA) (30 ng/mL)/ionomycin (0.75 μg/mL) or cell media as negative control were added to the Jurkat cells and incubated for 24 h. Supernatant samples (30 μL/well) were analyzed by ELISA using human IL-2 Ready-SET-Go ELISA kits from eBioscience (Hatfield, UK), according to the manufacturer's instructions.

https://dx.doi.org/10.1021/acs.bioconjchem.9b00799
Bioconjugate Chem. 2020, 31, 1107−1116

Absorbance at 450 and 570 nm was recorded using a SpectraMax 190 absorbance microplate reader, and mean absorbance of each sample at 450 nm was subtracted from absorbance at 570 nm. This protocol was repeated every other day for 6 days. The experiments were conducted in triplicates. Results are presented as the mean ± SD.

***In Vivo* PET Imaging and Biodistribution Studies.** All animal experiments complied with the ARRIVE guidelines, the Animals (Scientific Procedures) Act (UK 1986), and Home Office (UK) guidelines and were conducted under a Home Office license (P9C94E8A4) with local ethical approval by the KCL College Research Ethics Committee (CREC).

Preclinical PET/CT images were acquired using a Nano-Scan PET/CT (Mediso, Budapest, Hungary) scanner with mice under 2% isoflurane in oxygen anesthesia. Drinking water containing potassium iodide (0.1%, w/v) was provided to 6−7 week old male NSG mice (n = 7) for 1 week before and throughout the PET/CT imaging experiments. On day eight, they were randomly divided into two groups and received either the ^{124}I-FIT-$(PhS)_2$Mal [**2**] labeled Jurkat cells (∼0.5−1.0 × 10^7, ∼0.5−1.0 MBq, n = 3) in PBS or ^{124}I-FIT-$(PhS)_2$Mal [**2**] (∼0.7 MBq, n = 4) in PBS (100 μL) with 5% DMSO *via* tail vein injection. PET scanning was performed for 60 min either at 4, 24 h, 2, 4, and 7 days post Jurkat cell inoculation or at 24 h post ^{124}I-FIT-$(PhS)_2$Mal [**2**] injection followed by a 15 min CT scan. All PET/CT data were reconstructed with the Monte Carlo-based full-3D iterative algorithm Tera-Tomo (Mediso Medical Imaging Systems, Budapest, Hungary). Raw PET data were reconstructed into 60 min bins using reconstruction settings (4 iterations, 6 subsets, 0.4 × 0.4 × 0.4 mm^3 voxel size) as well as intercrystal scatter correction. All reconstructed data were analyzed with VivoQuant software (v3.0, inviCRO, LLC, Boston, USA). All animals were euthanized by cervical dislocation at the end of the last PET/CT scan. The major thoracoabdominal organs, brain, blood, urine, left femur, and thigh muscle were harvested, weighed, and gamma-counted. The radioactivity in each organ was expressed as % ID/g. The total injected dose was defined as the sum of the whole body counts excluding the tail.

Immunohistochemistry. Three cryosections (10 μm thick) were prepared from the liver and lung of NSG mice (n = 3) 1 week after receiving either ^{124}I-FIT-$(PhS)_2$Mal [**2**] labeled Jurkat cells from the above PET imaging study, PBS, or nonlabeled Jurkat cells (∼1.0 × 10^7). These tissue sections were fixed with acetone and dried in air. The tissue sections were then sequentially incubated with anti-CD3 primary antibody (clone LN10, Leica #CD3-565-L-CE) and Polymer-supported peroxidase and anti-Mouse IgG followed by DAB treatment (MaxVision2 HRP-Polymer anti-Mouse IHC Kit) and finally stained with hematoxylin. The tissue sections were then observed under an Olympus DP73 digital microscope.

■ ASSOCIATED CONTENT

Supporting Information

The Supporting Information is available free of charge at https://pubs.acs.org/doi/10.1021/acs.bioconjchem.9b00799.

HPLC chromatograms including crude radioiodination mixture of dual labeling reagents and coelution with their nonradioactive reference compounds; cell surface thiol determination; table for ^{124}I-FIT-$(PhS)_2$Mal [**2**] labeled Jurkat cell biodistribution data from NSG mice 7 days post IV injection; table for ^{124}I-FIT-$(PhS)_2$Mal [**2**] biodistribution data from NSG mice 24 h post IV injection; and ^{1}H and ^{13}C NMR spectra for all compounds prepared (PDF)

■ AUTHOR INFORMATION

Corresponding Author

Ran Yan − *School of Biomedical Engineering and Imaging Sciences, St. Thomas' Hospital, King's College London, London SE1 7EH, United Kingdom;* orcid.org/0000-0002-0303-3196; Phone: 00442071889613; Email: ran.yan@kcl.ac.uk

Authors

Truc Thuy Pham − *School of Biomedical Engineering and Imaging Sciences, St. Thomas' Hospital, King's College London, London SE1 7EH, United Kingdom*

Zhi Lu − *Department of Nuclear Medicine, First Affiliated Hospital of Dalian Medical University, Dalian 116020, People's Republic of China*

Christopher Davis − *School of Biomedical Engineering and Imaging Sciences, St. Thomas' Hospital, King's College London, London SE1 7EH, United Kingdom*

Chun Li − *Department of Nuclear Medicine, First Affiliated Hospital of Dalian Medical University, Dalian 116020, People's Republic of China*

Fangfang Sun − *Department of Nuclear Medicine, First Affiliated Hospital of Dalian Medical University, Dalian 116020, People's Republic of China*

John Maher − *School of Cancer and Pharmaceutical Studies, Guy's Hospital, King's College London, London SE1 9RT, United Kingdom; Department of Immunology, Eastbourne Hospital, Eastbourne BN21 2UD, United Kingdom; Department of Clinical Immunology and Allergy, King's College Hospital NHS Foundation Trust, London SE5 9RS, United Kingdom*

Complete contact information is available at: https://pubs.acs.org/10.1021/acs.bioconjchem.9b00799

Notes

The views expressed are those of the authors and not necessarily those of the NHS, the NIHR, or the DoH.

The authors declare the following competing financial interest(s): J.M. is Chief Scientific Officer of Leucid Bio, which is a spinout company focused on development of cellular therapeutic agents.

■ ACKNOWLEDGMENTS

T.T.P. received a Rosetrees Trust PhD studentship (M545) to support this work. Z.L. received funding from the Natural Science Foundation of Liaoning Province, China (20180530048) for support of this work. C.D. received an EPSRC PhD studentship (EP/R513064/1) to support this work. The research was funded/supported by the National Institute for Health Research (NIHR) Biomedical Research Centre based at Guy's and St. Thomas' NHS Foundation Trust and King's College London, the Wellcome/EPSRC Centre for Medical Engineering at King's College London [WT 203148/Z/16/Z], the King's College London and UCL Comprehensive Cancer Imaging Centre funded by CRUK and EPSRC in association with the MRC and DoH (England), the Experimental Cancer Medicine Centre at King's College, and the King's Health Partners/King's College London Cancer

Research UK Cancer Centre. PET scanning equipment was funded by an equipment grant from the Wellcome Trust.

■ ABBREVIATIONS

Bq, becquerel; CT, computed tomography; IV, intravenous; % ID/g, percentage injected dose per gram tissue; PBS, phosphate buffered saline; PET, positron emission tomography; NIS, *N*-iodosuccinimide; RCYs, radiochemical yields; RT, room temperature; TCEP, tris(2-carboxyethyl)phosphine; TEA·HCl, triethylamine hydrochloride

■ REFERENCES

(1) Hinrichs, C. S., and Rosenberg, S. A. (2014) Exploiting the Curative Potential of Adoptive T-Cell Therapy for Cancer. *Immunol. Rev. 257* (1), 56−71.
(2) Trounson, A., and McDonald, C. (2015) Stem Cell Therapies in Clinical Trials: Progress and Challenges. *Cell Stem Cell 17* (1), 11−22.
(3) Scalea, J. R., Tomita, Y., Lindholm, C. R., and Burlingham, W. (2016) Transplantation Tolerance Induction: Cell Therapies and Their Mechanisms. *Front. Immunol. 7*, 87.
(4) Feins, S., Kong, W., Williams, E. F., Milone, M. C., and Fraietta, J. A. (2019) An Introduction to Chimeric Antigen Receptor (CAR) T-Cell Immunotherapy for Human Cancer. *Am. J. Hematol. 94* (S1), S3−S9.
(5) Kircher, M. F., Gambhir, S. S., and Grimm, J. (2011) Noninvasive Cell-Tracking Methods. *Nat. Rev. Clin. Oncol. 8* (11), 677−688.
(6) Martinez, O., Sosabowski, J., Maher, J., and Papa, S. (2019) New Developments in Imaging Cell-Based Therapy. *J. Nucl. Med. 60* (6), 730−735.
(7) Hughes, D. K. (2003) Nuclear Medicine and Infection Detection: The Relative Effectiveness of Imaging with ^{111}In-Oxine-, ^{99m}Tc-HMPAO-, and ^{99m}Tc-Stannous Fluoride Colloid-Labeled Leukocytes and with ^{67}Ga-Citrate. *J. Nucl. Med. Technol. 31* (4), 196−201.
(8) Bulte, J. W. M. (2009) *In Vivo* MRI Cell Tracking: Clinical Studies. *AJR, Am. J. Roentgenol. 193* (2), 314−325.
(9) Swirski, F. K., Berger, C. R., Figueiredo, J. L., Mempel, T. R., von Andrian, U. H., Pittet, M. J., and Weissleder, R. (2007) A Near-Infrared Cell Tracker Reagent for Multiscopic *In Vivo* Imaging and Quantification of Leukocyte Immune Responses. *PLoS One 2* (10), e1075.
(10) Man, F., Lim, L., Volpe, A., Gabizon, A., Shmeeda, H., Draper, B., Parente-Pereira, A. C., Maher, J., Blower, P. J., Fruhwirth, G. O., et al. (2019) *In Vivo* PET Tracking of ^{89}Zr-Labeled Vγ9Vδ2 T Cells to Mouse Xenograft Breast Tumors Activated with Liposomal Alendronate. *Mol. Ther. 27*, 219−229.
(11) Weist, M. R., Starr, R., Aguilar, B., Chea, J., Miles, J. K., Poku, E., Gerdts, E., Yang, X., Priceman, S. J., Forman, S. J., et al. (2018) PET of Adoptively Transferred Chimeric Antigen Receptor T Cells with ^{89}Zr-Oxine. *J. Nucl. Med. 59* (10), 1531−1537.
(12) Sato, N., Wu, H., Asiedu, K. O., Szajek, L. P., Griffiths, G. L., and Choyke, P. L. (2015) (89)Zr-Oxine Complex PET Cell Imaging in Monitoring Cell-Based Therapies. *Radiology 275* (2), 490−500.
(13) Charoenphun, P., Meszaros, L. K., Chuamsaamarkkee, K., Sharif-Paghaleh, E., Ballinger, J. R., Ferris, T. J., Went, M. J., Mullen, G. E. D., and Blower, P. J. (2015) [^{89}Zr]Oxinate$_4$ for Long-Term in Vivo Cell Tracking by Positron Emission Tomography. *Eur. J. Nucl. Med. Mol. Imaging 42* (2), 278−287.
(14) Bansal, A., Pandey, M. K., Demirhan, Y. E., Nesbitt, J. J., Crespo-Diaz, R. J., Terzic, A., Behfar, A., and DeGrado, T. R. (2015) Novel ^{89}Zr Cell Labeling Approach for PET-Based Cell Trafficking Studies. *EJNMMI Res. 5*, 19.
(15) Belov, V. V., Bonab, A. A., Fischman, A. J., Heartlein, M., Calias, P., and Papisov, M. I. (2011) Iodine-124 as a Label for Pharmacological PET Imaging. *Mol. Pharmaceutics 8*, 736−747.
(16) Kim, H., Shin, K., Park, O. K., Choi, D., Kim, H. D., Baik, S., Lee, S. H., Kwon, S.-H., Yarema, K. J., Hong, J., et al. (2018) General and Facile Coating of Single Cells via Mild Reduction. *J. Am. Chem. Soc. 140* (4), 1199−1202.
(17) Stephan, M. T., Moon, J. J., Um, S. H., Bershteyn, A., and Irvine, D. J. (2010) Therapeutic Cell Engineering with Surface-Conjugated Synthetic Nanoparticles. *Nat. Med. 16* (9), 1035−1041.
(18) Schumacher, F. F., Nunes, J. P. M., Maruani, A., Chudasama, V., Smith, M. E. B., Chester, K. A., Baker, J. R., and Caddick, S. (2014) Next Generation Maleimides Enable the Controlled Assembly of Antibody-Drug Conjugates via Native Disulfide Bond Bridging. *Org. Biomol. Chem. 12* (37), 7261−7269.
(19) Schumacher, F. F., Nobles, M., Ryan, C. P., Smith, M. E. B., Tinker, A., Caddick, S., and Baker, J. R. (2011) In Situ Maleimide Bridging of Disulfides and a New Approach to Protein PEGylation. *Bioconjugate Chem. 22* (2), 132−136.
(20) Yan, R., El-Emir, E., Rajkumar, V., Robson, M., Jathoul, A. P., Pedley, R. B., and Årstad, E. (2011) One-Pot Synthesis of an ^{125}I-Labeled Trifunctional Reagent for Multiscale Imaging with Optical and Nuclear Techniques. *Angew. Chem., Int. Ed. 50* (30), 6793−6795.
(21) Yan, R., Sander, K., Galante, E., Rajkumar, V., Badar, A., Robson, M., El-Emir, E., Lythgoe, M. F., Pedley, R. B., and Årstad, E. (2013) A One-Pot Three-Component Radiochemical Reaction for Rapid Assembly of ^{125}I-Labeled Molecular Probes. *J. Am. Chem. Soc. 135* (2), 703−709.
(22) Lu, Z., Pham, T. T., Rajkumar, V., Yu, Z., Pedley, R. B., Årstad, E., Maher, J., and Yan, R. (2018) A Dual Reporter Iodinated Labeling Reagent for Cancer Positron Emission Tomography Imaging and Fluorescence-Guided Surgery. *J. Med. Chem. 61*, 1636−1645.
(23) Lakouraj, M. M., and Ghodrati, K. (2008) A Facile and Convenient Method for the Conversion of Thioamides into Amides Using Pyridinium Hydrobromide Perbromide. *Monatsh. Chem. 139*, 549−551.
(24) Castañeda, L., Wright, Z. V. F., Marculescu, C., Tran, T. M., Chudasama, V., Maruani, A., Hull, E. A., Nunes, J. P. M., Fitzmaurice, R. J., Smith, M. E. B., et al. (2013) A Mild Synthesis of *N*-Functionalised Bromomaleimides, Thiomaleimides and Bromopyridazinediones. *Tetrahedron Lett. 54* (27), 3493−3495.
(25) Sahu, S., Rani Sahoo, P., Patel, S., and Mishra, B. K. (2011) Oxidation of thiourea and substituted thioureas: a review. *J. Sulfur Chem. 32* (2), 171−197.
(26) Li, L., Han, B., Wang, Y., Zhao, J., and Cao, Y. (2019) Simple and Universal Signal Labeling of Cell Surface for Amplified Detection of Cancer Cells Via Mild Reduction. *Biosens. Bioelectron. 145*, 111714.
(27) Tracking Peripheral Immune Cell Infiltration of the Brain in Central Inflammatory Disorders Using [Zr-89]Oxinate$_4$-labeled Leukocytes. https://clinicaltrials.gov/ct2/show/NCT03807973 (accessed 2020-03-09).
(28) Sato, N., Stringaris, K., Davidson-Moncada, J. K., Reger, R., Adler, S. S., Dunbar, C., Choyke, P. L., and Childs, R. W. (2020) In-vivo tracking of adoptively transferred natural killer-cells in rhesus macaques using ^{89}Zirconium-oxine cell labeling and PET imaging. *Clin. Cancer Res.*, DOI: 10.1158/1078-0432.CCR-19-2897.
(29) Badawi, R. D., Shi, H., Hu, P., Chen, S., Xu, T., Price, P. M., Ding, Y., Spencer, B. A., Nardo, L., Liu, W., Bao, J., Jones, T., Li, H., and Cherry, S. R. (2019) First Human Imaging Studies with the EXPLORER Total-Body PET Scanner. *J. Nucl. Med. 60* (3), 299−303.